



Article

Beta-Secretase 1 Recruits Amyloid-Beta Precursor Protein to ROCK2 Kinase, Resulting in Erroneous Phosphorylation and Beta-Amyloid Plaque Formation

István Hajdú ^{1,*}, Barbara M. Végh ^{1,†}, András Szilágyi ¹ and Péter Závodszy ^{1,2,*}

¹ Institute of Enzymology, Research Centre for Natural Sciences, 1117 Budapest, Hungary; vech.barbara@ttk.hu (B.M.V.); szilagyi.andras@ttk.hu (A.S.)

² Faculty of Information Technology and Bionics, Pázmány Péter Catholic University, 1083 Budapest, Hungary

* Correspondence: hajdu.istvan@ttk.hu (I.H.); zavodszy.peter@ttk.hu (P.Z.)

† These authors contributed equally to this work.

Abstract: The amyloidogenic processing of APP depends on two events: its phosphorylation by ROCK2 (at Thr654) and the phosphorylation of the APP-cleaving enzyme BACE1 (at Ser498). However, the mechanisms and structural details of APP-ROCK2 and BACE1-ROCK2 binding are unknown. Using direct physical methods in combination with an in silico approach, we found that BACE1 binds into the substrate-binding groove of ROCK2 with a low affinity ($K_d = 18 \mu\text{M}$), while no binding of APP to ROCK2 alone could be detected. On the other hand, a strong association ($K_d = 3.5 \text{ nM}$) of APP to the weak ROCK2-BACE1 complex was observed, although no stable ternary complex was detected, i.e., BACE1 was displaced by APP. We constructed a sequential functional model: (1) BACE1 weakly binds to ROCK2 and induces an allosteric conformational change in ROCK2; (2) APP strongly binds to the ROCK2-BACE1 complex, and BACE1 is released; and (3) ROCK2 phosphorylates APP at Thr654 (leading to a longer stay in the early endosome during APP processing). Direct fluorescence titration experiments showed that the APP_{646–664} or APP_{665–695} fragments did not bind separately to the ROCK2-BACE1 complex. Based on these observations, we conclude that two binding sites are involved in the ROCK2-APP interaction: (1) the substrate-binding groove, where the APP_{646–664} sequence containing Thr654 sits and (2) the allosteric binding site, where the APP_{665–695} sequence binds. These results open the way to attack the allosteric site to prevent APP phosphorylation at Thr654 by ROCK2 without inhibiting the activity of ROCK2 towards its other substrates.

Keywords: rho-kinase (ROCK); phosphorylation; amyloid precursor protein (APP); beta-secretase (BACE1); allosteric binding site



Citation: Hajdú, I.; Végh, B.M.; Szilágyi, A.; Závodszy, P. Beta-Secretase 1 Recruits Amyloid-Beta Precursor Protein to ROCK2 Kinase, Resulting in Erroneous Phosphorylation and Beta-Amyloid Plaque Formation. *Int. J. Mol. Sci.* **2023**, *24*, 10416. <https://doi.org/10.3390/ijms241310416>

Academic Editor: Dorian Fabbro

Received: 31 May 2023

Revised: 13 June 2023

Accepted: 16 June 2023

Published: 21 June 2023



Copyright: © 2023 by the authors. Licensee MDPI, Basel, Switzerland. This article is an open access article distributed under the terms and conditions of the Creative Commons Attribution (CC BY) license (<https://creativecommons.org/licenses/by/4.0/>).

1. Introduction

Alzheimer's disease is currently the leading cause of dementia, with no effective treatment. Evidence indicates that the amyloid precursor protein (APP) and its derivative, amyloid- β ($A\beta$) peptide, play an important role in its development [1]. Although $A\beta$ cannot account for all features of Alzheimer's disease, reducing $A\beta$ production or accumulation is a major therapeutic strategy to confront the disease [2]. The accumulation of $A\beta$ peptides in senile plaques is the consequence of pathological processing of APP. There are two major pathways of APP processing: a non-amyloidogenic pathway involving α -secretase [3], and an amyloidogenic pathway involving the primary cleavage of APP by β -secretase [4]. Both pathways include the subsequent action of γ -secretases [5]. The relative contribution of each pathway to the whole processing mainly depends on the subcellular localization of the process: the amyloidogenic pathway typically occurs in the early endosome [6], where the acidic environment favors the proteolytic activity of β -secretase, also known as β -site APP-cleaving enzyme 1 (BACE1), accounting for the β -cleavage. The APP protein (like other proteins) undergoes trafficking between the different subcellular components. It was

shown that phosphorylation of the intracellular domain of the APP modifies its trafficking behavior [7]. The phosphorylation of Thr654 by ROCK2 extends the residence time of APP in the early endosome, which leads to a higher probability of A β formation. Interestingly, it was also demonstrated that the phosphorylation of BACE1 at Ser498 by ROCK2 also prolongs its residence time in the early endosome. Based on these results, it is assumed that pharmacological inhibition of ROCK2 could suppress A β production by interfering with two different pathways in parallel. It was demonstrated that specific inhibition of ROCK2 using an isoform-selective small molecule (SR3677) diminished the production of A β in an AD mouse brain via the two mechanisms [8]. Although this molecule leaves ROCK1 activity unmodified [9], the vast number of ROCK2 functions make this kind of specific but activity-targeted inhibition prone to side effects [10].

ROCK2 is a large, 1388-residue-long multidomain dimeric serine/threonine kinase localized in the cytoplasm of cells anchored to the plasma membrane by their C-terminal regions [11] (Figure 1). The C-terminal region contains a lipid-binding split pleckstrin homology domain which is bisected by an internal cysteine-rich zinc-finger domain. The center of the molecule forms a long coiled-coil domain containing the Rho-binding domain. The catalytic (kinase) domain is located at its N-terminus. Although the structure of the whole molecule is only known at low resolutions [12], it is evident that for enzymatic activity, only the kinase domains are required. Recently, we constructed a functional model to explain the membrane-proximal and membrane-distal activities of ROCK2, where the weak complex between its terminal domains can be dissociated by natural substrates, allowing the kinase domain to access the substrate [13]. The concept of the present study is based on this model.

APP is a type I integral membrane glycoprotein widely expressed both in neuronal and non-neuronal cells having at least three isoforms with different lengths [14]. In the brain, the amyloidogenic 695-residue-long APP₆₉₅ is the most prominent isoform [15], which is preferentially processed to generate A β . In the amyloidogenic pathway, APP is first cleaved by BACE1, releasing the soluble ectodomain region of APP (sAPP β) [16]. The remaining 99-residue C-terminal fragment is cleaved at the ϵ -site by γ -secretase, releasing the 50-residue-long APP intracellular domain [17] and the A β fragment; A β is then further processed at the ζ - [18] and γ -sites [19] by γ -secretase to yield the A β ₄₀ and A β ₄₂ final products. The intracellular domain of APP contains a number of phosphorylation sites (Tyr653 [20], Thr654 [8], Ser655 [21,22], Thr668 [23–27], Ser675 [28], Tyr682 [29,30], Thr686 [20] and Tyr687 [31]), which are all phosphorylated to various degrees in the brain of patients with Alzheimer's disease in contrast to healthy brains, suggesting that the phosphorylation events may have a significant impact on the physiological function of APP.

BACE1 is an aspartyl protease of the pepsin family. BACE1 is a type I transmembrane protein, having an extracellular protease domain, a short transmembrane domain and a short 23-residue cytoplasmic C-terminal domain [32]. BACE1 is widely expressed in the brain, particularly in neurons, oligodendrocytes and astrocytes. At the subcellular level, BACE1 localizes on the plasma membrane and in the endosomal compartments, and has been detected in healthy synaptic terminals and dystrophic neurites surrounding amyloid- β plaques [33]. Post-translational modifications of BACE1 are known; its phosphorylation (mainly at Ser498) is important for cellular trafficking [34], although exactly how the phosphorylation of Ser498 modifies the trafficking pathways is controversial [8,35].

In our study, we focus on the mechanism of APP and BACE1 binding by ROCK2, and the aim is the localization and mapping of the protein–protein interaction sites between these proteins to create the basis for the design or selection of allosteric inhibitors targeting A β production.

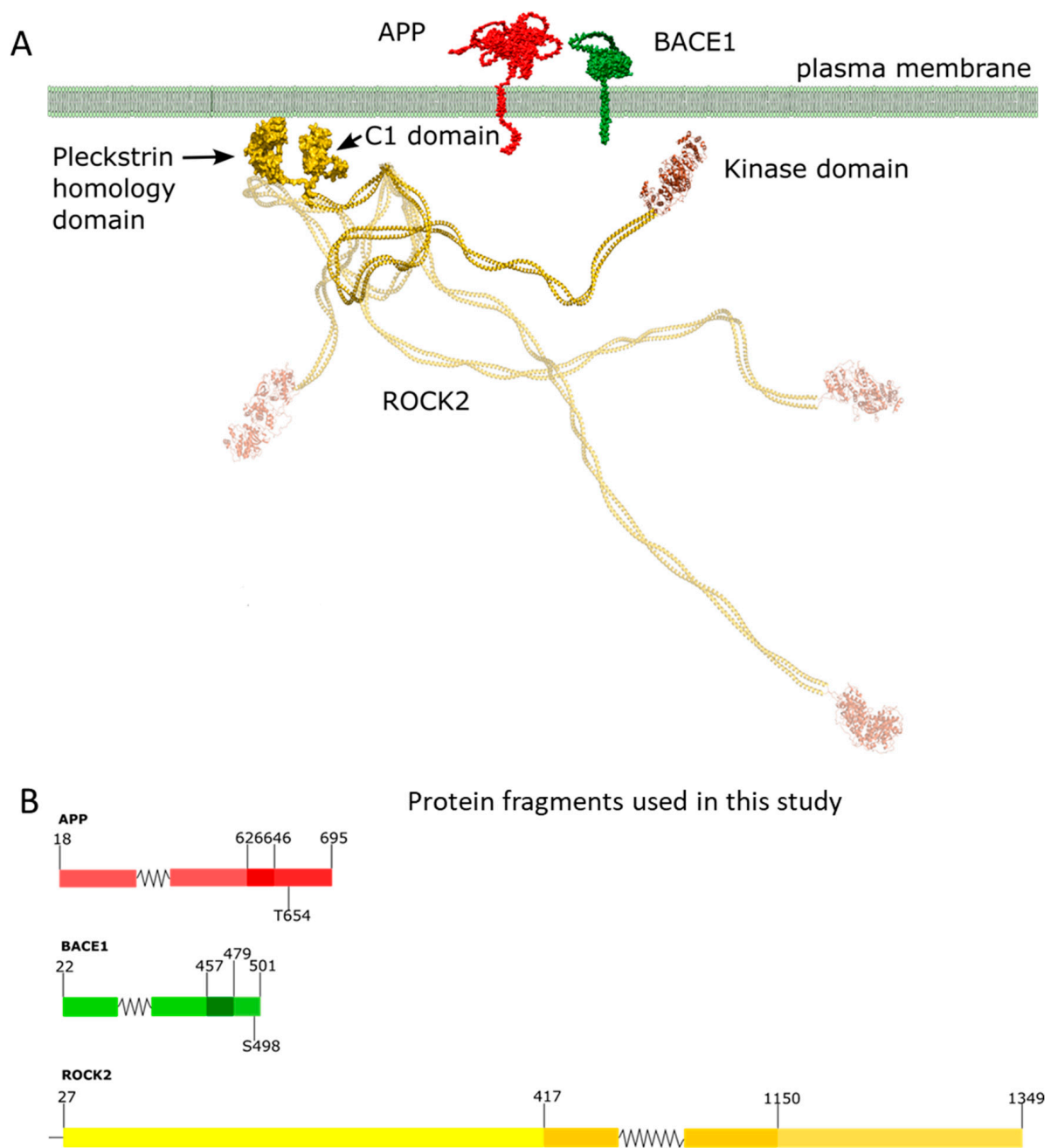


Figure 1. Domain structure, membrane topology and cellular localization of ROCK2, BACE1 and APP. ROCK2 is anchored to the plasma membrane by its C-terminal region, through its split pleckstrin domain bisected by a C1 domain. Both BACE1 and APP are transmembrane proteins with short (23 and 50 residues, respectively) intracellular C-terminal domains (**panel A**). In (**panel B**), we show the expressed protein fragments; in the case of APP, the C-terminal intracellular domain from 646 to 695 was the largest fragment, which comprises the phosphorylatable Thr654. The peptide representing the BACE1 C-terminal intracellular domain (residues 479–501) was used. In the case of ROCK2, the full-length version and the kinase domain (residues 27–417) was used. Schemes follow the same formatting. (**Panel A**) is a modification of our previous image [13], while panel B was edited using Inkscape 1.2 (Inkscape Project. (2020). Inkscape. Retrieved from <https://inkscape.org>, accessed on 13 May 2023).

To reveal the structural features of the interaction, we produced the relevant domains of ROCK2, APP and BACE1, either in recombinant or synthetic forms. Using biophysical methods (including surface plasmon resonance and fluorescence resonance) and structural modeling, we identified the protein–protein interactions and constructed a model for the mechanism of cooperation between these three proteins.

The accumulation of A β -peptides in senile plaques—observed in Alzheimer’s disease—is the consequence of erroneous processing of APP. The cause of this is the erroneous phosphorylation of APP and BACE1 by ROCK2. Our goal is to reveal the mechanistic and structural features of the phosphorylation process of BACE1 and APP by ROCK2.

2. Results

2.1. BACE1-ROCK2 Binary Interaction

We used surface plasmon resonance to examine the binary binding properties between ROCK2 and its partners. Full-length ROCK2 protein was immobilized on a chip and used as the ligand using a high-density surface of 1700 resonance units. The binding of the BACE1 cytoplasmic domain (BACE1CD) to ROCK2 was only detected at a significant 15-fold molar excess of ATP (Figure 2A). Considering the molecular weights of the ligand (ROCK2) and the analyte, the signal (11 resonance units, RUs) was approximately 50% of the theoretical signal (23 RUs, based on the molecular weight ratio of the analyte and the ligand and the quantity of the immobilized ligand), which implies that half of the bound ROCK2 molecules bind BACE1. As amine coupling is a random binding method, the 50% binding is near the maximum possible signal expected. The exact binding parameters could not be determined, primarily due to the low signal and the high ligand density.

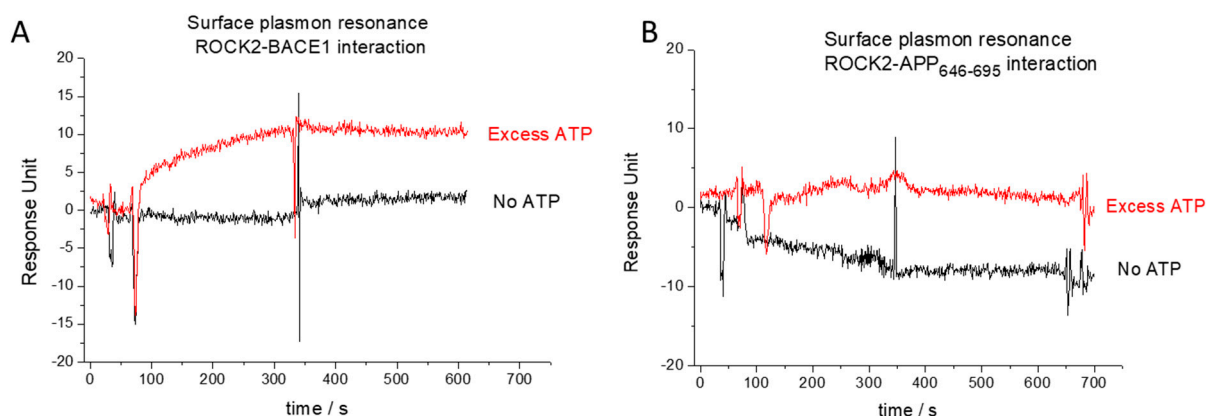


Figure 2. Surface plasmon resonance analysis of binary interaction between ROCK2 and its ligands. Weak interaction was detected between ROCK2 and BACE1 only in the presence of excess ATP (red curve on (panel A)), while this interaction was not observed without ATP (black curve on (panel B)). No binary interaction was detected between ROCK2 and APP_{646–695}, either in the presence (red curve on (panel B)) or absence of ATP (black curve on (panel B)).

To quantify the binding affinity between ROCK2 and BACE1, fluorescence polarization measurements were used. The affinity of the binding between either the kinase domain or full-length ROCK2 and fluorescein-labeled C-terminal BACE1 peptide was calculated from a direct measurement using a known concentration (50 nM) of labeled BACE1 and a dilution series for ROCK2. The calculated dissociation constant (K_d) was 18 μ M (Figure 3A) for both the kinase domain and the full-length ROCK2. This indicates that there is a direct interaction between BACE1 and ROCK2, but the binding is weak and is independent of the N-terminal region.

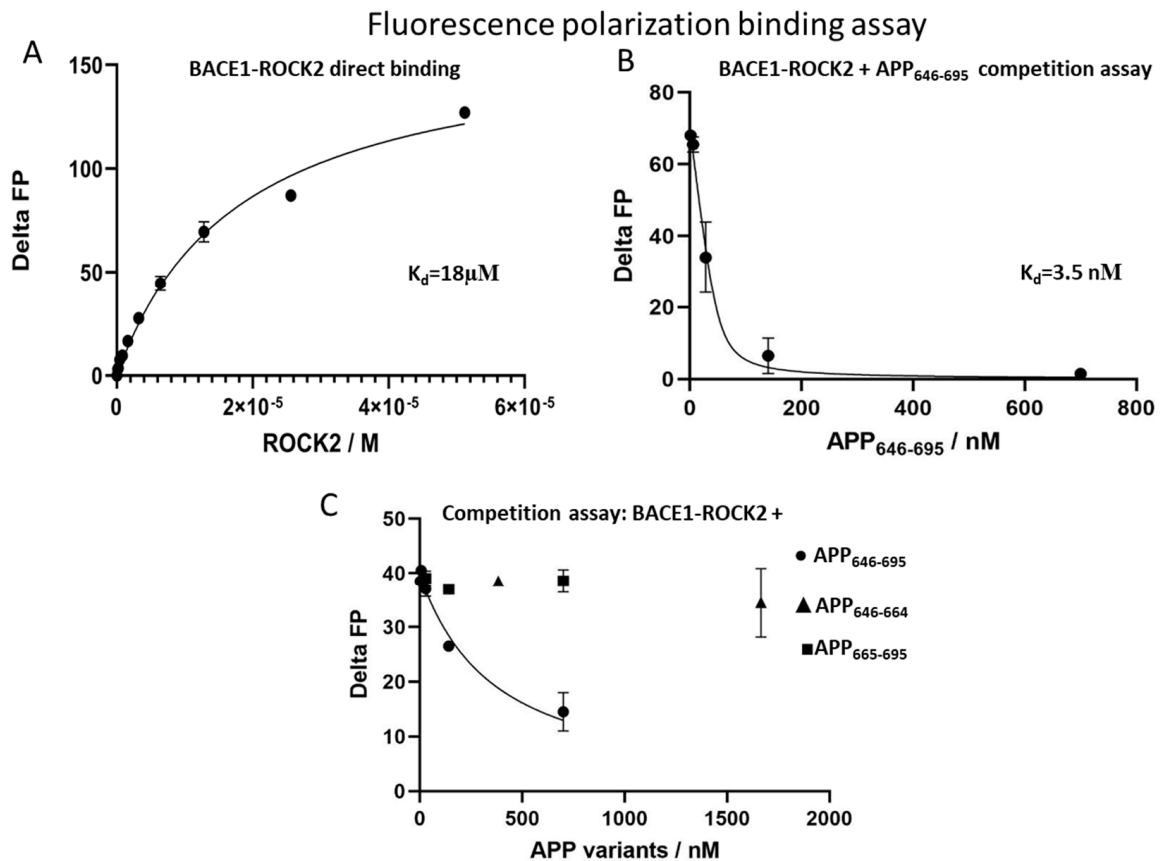


Figure 3. Detection of interactions by fluorescence polarization. Direct titration of fluorescein-labeled BACE1 with ROCK2 showed a binding constant of 18 μM (panel A). Competition of the ROCK2-BACE1 interaction with APP₆₄₆₋₆₉₅, showing an interaction constant of 3.3 nM using a fixed BACE1 concentration of 50 nM (panel B). The fragments APP₆₄₆₋₆₆₄ (triangles) and APP₆₆₅₋₆₉₅ (squares) do not displace BACE1 from ROCK2, only doing so for APP₆₄₆₋₆₉₅ (circles) (panel C).

2.2. APP-ROCK2 Binary Interaction

Using the same approaches as for ROCK2-BACE1 binding, no binding could be detected between ROCK2 and APP. Surface plasmon resonance experiments did not show binding either with or without ATP added (Figure 2B). In the fluorescence polarization studies, we used C-terminal TAMRA (5-Carboxytetramethylrhodamine)-labeled APP₆₄₆₋₆₉₅ peptides. The use of TAMRA was useful, as its polarizable fluorescence spectrum is readily distinguishable from that of fluorescein. The polarization signal was unchanged, even using the highest available concentration (6 μM) of ROCK2, indicating the lack of direct binary interactions between ROCK2 and APP.

2.3. In Search of a ROCK2-BACE1-APP Ternary Interaction

Our finding that the C-terminal domain of APP did not bind to ROCK2 is in contradiction with previous studies [8], indicating that ROCK2 can phosphorylate full-sized APP. To resolve this problem, we assumed that an extra partner is required for the interaction, and the most relevant interaction partner might be BACE1 itself. Since we know that BACE1 and APP are in close proximity in cells [36], we turned to investigating the ternary interactions between ROCK2, BACE1 and APP₆₄₆₋₆₉₅.

As the binding of fluorescein-labeled BACE1 to ROCK2 can easily be monitored in fluorescence polarization assays, we designed a competition fluorescence polarization assay using fixed amounts of ROCK2 and labeled BACE1. When adding APP₆₄₆₋₆₉₅ to the ROCK2-labeled BACE1 mix, a high-affinity interaction with a K_d of 3.5 nM was found (Figure 3B).

We have shown that the 646–695 sequence of APP binds to ROCK2 in the presence of BACE1. It is known that APP_{646–695} is composed of an unstructured stretch (APP_{646–664}) and a globular domain (APP_{665–695}) [37]. For a more detailed structural mapping of the APP binding site on ROCK2, we studied the binding of both the APP_{646–664} and the APP_{665–695} fragments. The competition assay against ROCK2-BACE1 revealed that neither fragment of APP_{646–695} was capable of displacing BACE1 from ROCK2 (Figure 3C). This result indicates that the full 50-residue segment of APP is required for high-affinity binding to the ROCK2/BACE1.

To identify the binding position of ligands on ROCK2, the structures of the binary complexes were modeled with AlphaFold [38]. The binding site for both BACE1 and APP is composed mainly of the canonical kinase substrate-binding groove (Figure 4), with the C-terminal tail of APP_{646–695} making contacts with two additional helices on the ROCK2 kinase domain. Both ligands appear to occupy the binding groove; therefore, a ternary complex between the three proteins is improbable, as was proved experimentally.

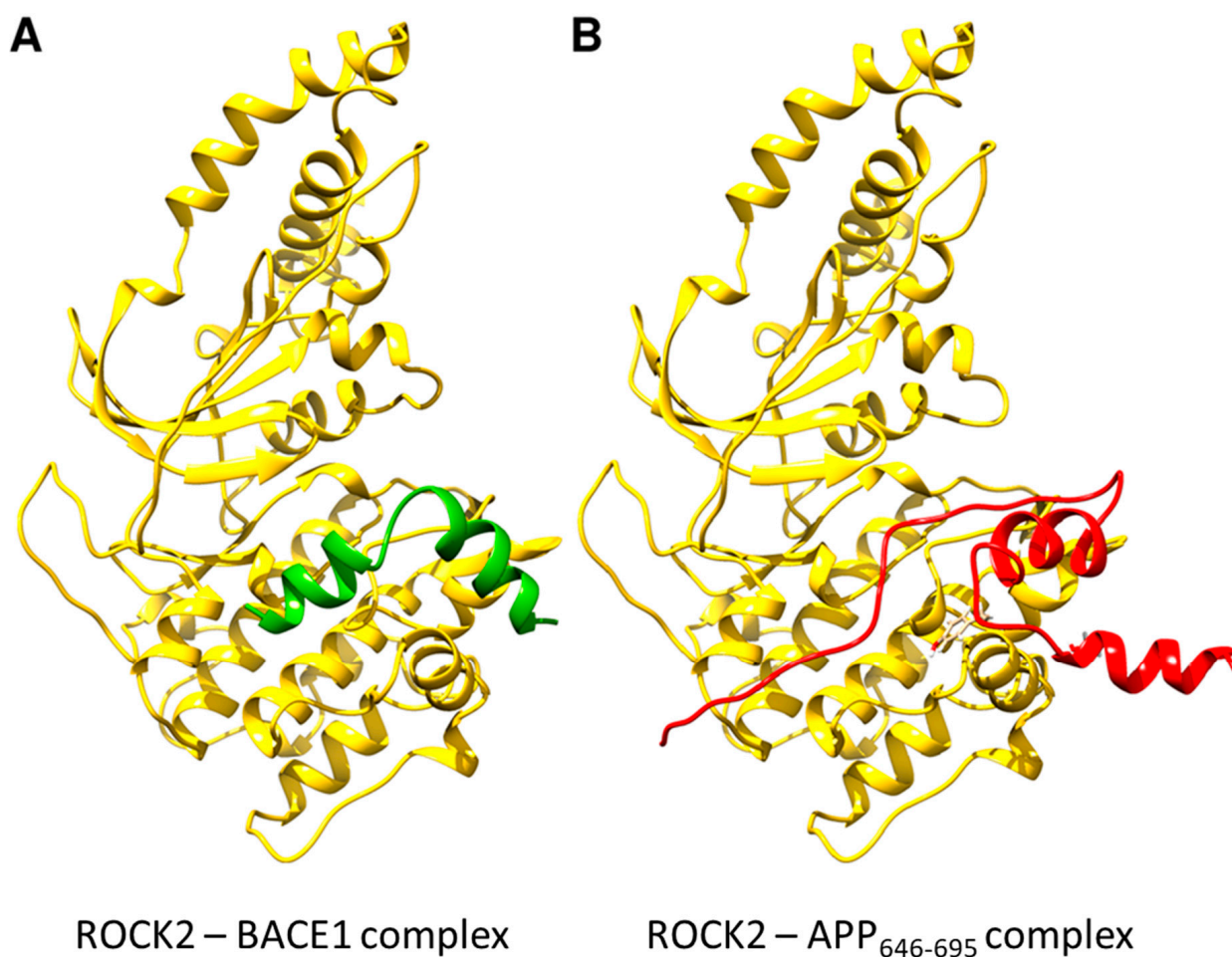


Figure 4. Structures of ROCK2-BACE1 (A) and ROCK2-APP_{646–695} (B) complexes as predicted using AlphaFold-Multimer. ROCK2 is shown in yellow, BACE1 in green and APP_{646–695} in red. The binding site for both BACE1 and APP is composed of mainly the canonical kinase substrate-binding groove, with the C-terminal tail of APP_{646–695} making contacts with two additional helices on the ROCK2 kinase domain. Structures of ROCK2-BACE1 and ROCK2-APP_{646–695} complexes were predicted using AlphaFold-Multimer [39] as implemented in ColabFold [40].

3. Discussion

Despite decades of intensive research, there is no efficient drug to prevent or cure Alzheimer's disease. The amyloid hypothesis of the disease suggests that inhibiting A β production could reduce symptoms and slow disease progression. During the processing of APP, its cleavage by BACE1 is the rate-limiting step [16]; therefore, the inhibition of BACE1 could be a trivial solution. The development of small molecular inhibitors against BACE1 was set back with a series of unwanted side effects [41]. Previously, it was shown that pharmacological inhibition of ROCK2 activity diminishes sAPP β production as well as A β levels [8] by inhibiting the phosphorylation of Ser498 of BACE1 and Thr654 of APP, altering the endocytic traffic of both proteins. However, direct inhibition of ROCK2 kinase activity would be a risky approach because of the diverse physiological roles of ROCK2 [42,43]. The recent approval of belumosudil, a highly selective, low-molecular-weight ROCK2 inhibitor against chronic graft-versus-host disease [44] also indicates the multiple functional roles of ROCK2, although a recent study [45] suggested that the therapeutic effectiveness of belumosudil was partially due to inhibition of the protein kinase CK2 α . We believe that by avoiding side effects, pathway-specific inhibitors could provide a solution for the reduction in A β levels. This prompted us to study the molecular mechanism of the phosphorylation of BACE1 and APP by ROCK2 and map the protein–protein interactions involved.

Both BACE1 and APP are transmembrane proteins with short intracellular tails, while ROCK2 is an intracellular protein anchored to the membrane through its C-terminal regulatory domains. To avoid having to work with the full-sized proteins, we simplified the problem to those domains of the proteins which are in the same compartment, namely the C-terminal tails of BACE1 and APP, alongside ROCK2 kinase.

To understand the molecular mechanism of interaction between ROCK2 and its protein ligands, several lines of protein–protein interaction studies were undertaken. Our results clearly indicated the direct, although weak, interaction between ROCK2 and the C-terminal tail of BACE1. We could not detect a binary interaction between ROCK2 and APP_{646–695}. However, in the presence of BACE1, high-affinity interactions of ROCK2 and APP_{646–695} were observed.

Based on the binding experiments, we constructed a sequential model (Figure 5) for the mechanism of ROCK2 action on BACE1 and APP. In this model, BACE1 recruits APP to ROCK2 for phosphorylation. In the native conformation of ROCK2, BACE1 binds in the binding groove of ROCK2 [46], and this binding event drives a conformational change in ROCK2, inducing a new allosteric binding site. ROCK2 can interact with APP_{646–695} in this new conformation through a dual binding site, where the newly formed allosteric site binds the C-terminal (665–695) region of APP_{646–695}, while the binding groove of ROCK2 binds the N-terminal part, displacing BACE1. ROCK2 can now phosphorylate APP at Thr654, and phospho-APP dissociates, while ROCK2 is converted back to its original, native conformation. Alternatively, if APP is not available to displace BACE1 from ROCK2, ROCK2 can phosphorylate BACE1, which then dissociates.

This highly cooperative action between ROCK2, APP and BACE1 is in accordance with previous results indicating that the physical proximity of BACE1 and APP on the cell membrane is a main determining factor leading to the amyloidogenic pathway of APP processing [47,48].

Our results prove that the allosteric inhibition of the phosphorylation of APP by ROCK2 is a new, feasible option in the fight against Alzheimer's disease. Site-directed mutagenesis experiments are in progress to localize and map the relevant orthosteric and allosteric sites.

The „ping-pong like” mechanism of ROCK2 - BACE1 – APP₆₄₆₋₆₉₅ interaction

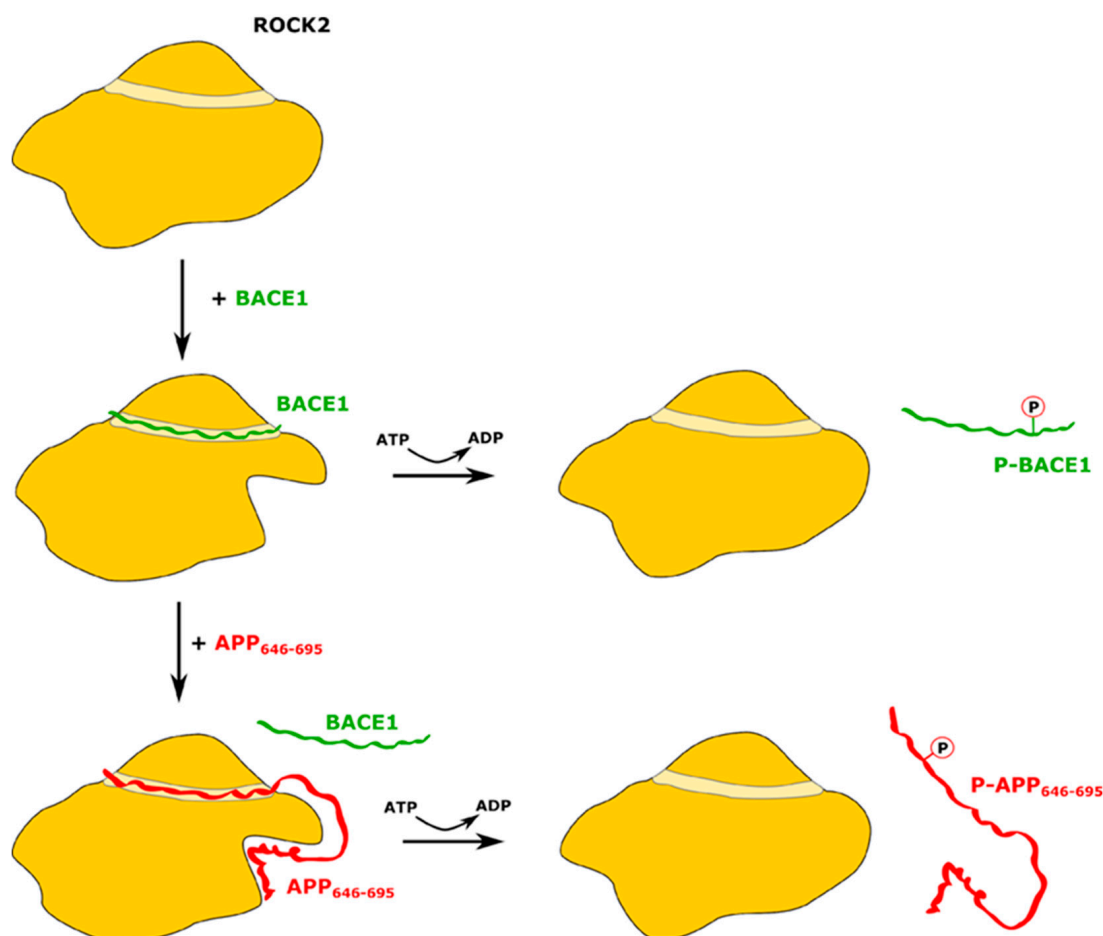


Figure 5. Scheme of the proposed ping-pong-like mechanism for the interaction and phosphorylation of BACE1 and APP by ROCK2 kinase. The kinase domain presents a canonical substrate-binding groove where the C-terminal peptide of BACE1 can bind. Upon the binding of BACE1, a conformational change occurs, creating a new allosteric binding site on ROCK2, which APP can interact with. The phosphorylation of BACE1 and the dissociation of p-BACE1 restores the initial state of ROCK2. When APP binds to the distorted ROCK2, BACE1 dissociates without the phosphorylation event but ROCK2 can phosphorylate APP. The dissociation of p-APP leads to the original ROCK2 conformation.

4. Materials and Methods

4.1. Protein Expression and Purification

The synthetic gene (Genent AG, Regensburg, Germany) of human APP₆₄₆₋₆₉₅ was cloned into the pONE10K [49] vector between NheI and NotI cleavage sites, using primers 5'-GGGCTAGCGTGATGCTGAAGAAGAAACAG-3' and 5'-GGGCGGCCGCCTAGCAGT-TCTGCATCTGCTCAAA-3'. The APP₆₄₆₋₆₆₄ construct was prepared using primers 5'-GCGCATATGAAAATCGAAGAAGGTAAACTGG-3' and 5'-GCGGCGGCCGCCTAGTCA-ACCTCCACCACACCATGATG-3', cloned between NdeI and NotI restriction sites. The APP₆₆₅₋₆₉₅ truncated construct was constructed using the QuikChange Site-Directed Mutagenesis Kit (Agilent Technologies, Santa Clara, CA, USA) protocol using the following oligos: 5'CCTGTA CTTC CAGGCCGCTGTCACCCC-3' and 5'-GGGGTGACAGCGGCCTGGA-AGTACAGG-3'. All primers used in this study were synthesized by Microsynth AG, Balgach, Switzerland.

The fusion protein constructs for the various APP peptides (containing maltose-binding protein (MBP) tag, which is a double-purpose expression tag, both enhancing protein expression and enabling amylose–resin-based affinity purification) [50] were transformed into Rosetta2 E. coli cells (Sigma-Aldrich, Burlington, MA, USA). The proteins were expressed at 37 °C in the presence of 50 µg/mL kanamycin and 30 µg/mL chloramphenicol. Protein expression was induced by adding 1 mM Isopropyl β-d-1-thiogalactopyranoside to the cell cultures upon reaching an OD₆₀₀ density of ~0.6–0.8. Before induction, cultures were equilibrated to an induction temperature of 21 °C for 0.5 h. Protein expression was continued overnight at 21 °C and 220 rpm. The MBP-tagged proteins were purified using amylose affinity chromatography. The cells were suspended in 25 mM of HEPES with a pH of 7.4, 500 mM NaCl and 1 mM dithiothreitol (DTT). The bound proteins were eluted by a buffer containing 10 mM maltose. The collected protein fractions were applied to a Superdex 75 gel filtration column equilibrated in 25 mM HEPES with a pH of 7.4, 150 mM NaCl and 1 mM DTT. Peak fractions were pooled and concentrated. The purity of proteins was tested using sodium dodecyl sulphate–polyacrylamide gel electrophoresis (SDS-PAGE) stained with Coomassie Brilliant Blue. All proteins were concentrated and stored at –20 °C.

The synthetic gene of human ROCK2 (1–1388) was cloned into the pONE30A vector between NheI and NotI cleavage sites. The ROCK2 kinase domain (27–417) construct (ROCK2-KD) truncation was prepared using primers 5'-GATCGCTAGCCAGAGGAAGCTGGAGGC-3' and 5'-GATCGCGGCCGCTCTATAGTAGGTAATCCGATG-3' and cloned into the pONE30A vector between NdeI and NotI restriction sites. Both protein constructs (containing MBP tags at the N-terminus) were expressed in Sf9 insect cells after co-transfection using flashBAC GOLD baculoviral expression system (Oxford Expression Technologies, Oxford, UK). After virus amplification, insect cells at 2 × 10⁶ cell/mL density were transfected with the recombinant baculovirus to express the protein of interest in 500 mL Insect-XPress medium (Lonza, Basel, Switzerland) for 3 days at 27 °C in a shaker flask at 220 rpm. The proteins were purified using amylose affinity chromatography in 25 mM HEPES with a pH of 7.4, 500 mM NaCl and 1 mM DTT. The bound proteins were eluted by a buffer containing 10 mM maltose. The collected protein fractions were dialyzed and concentrated against 25 mM HEPES buffer (pH 7.4) [13].

4.2. Peptides

For the studies, the reporter peptide, BACE1 (QWCLRLRQQHDDFADDISLLK), both in free form and N-terminally labeled with 5-FAM (5-Carboxyfluorescein), was purchased from GenScript (Piscataway, NJ, USA).

4.3. Fluorescence Labeling

APP_{646–695} was labeled with TAMRA (T6027 Invitrogen, Waltham, MA, USA) according to the following procedure: 5-Carboxytetramethylrhodamine dissolved dye was added in 2-fold molar excess to a purified APP_{646–695} sample and then incubated in the dark for 2 h at room temperature. Unreacted dye was removed on Ultracel-10K centrifugal filters (Sigma-Aldrich, Burlington, MA, USA). For enzyme activity, the MBP tag was removed using tobacco etch virus protease cleavage. The cleavage was performed in a 20-time molar excess of TEV protease at room temperature for 2 h. The APP_{646–695}-TAMRA constructs were separated from MBP using amylose affinity chromatography. The flowthrough was applied to a Superdex 75 gel filtration column equilibrated in 20 mM HEPES with a pH of 7.4, 150 mM NaCl and 1.5 mM EDTA. Peak fractions were pooled and concentrated. The purity of proteins was tested by SDS-PAGE stained with Coomassie Brilliant Blue and determined as ≥90% pure. The APP_{646–695}-TAMRA was concentrated and stored at –20 °C.

4.4. Fluorescence Polarization

Changes in the FP signal in direct binding affinity measurements were monitored as a function of the increasing concentration of purified APP variants with a Synergy H4 (Agilent, Santa Clara, CA, USA) plate reader in 384-well plates. The labeled peptides were at 10 nM in 20 mM Tris with a pH of 8.0, 100 mM NaCl, 0.05% Brij35P and 2 mM DTT. The affinities of the unlabeled peptides or different APP constructs to ROCK2 were measured in steady-state competition experiments, as follows: 50 nM (or 1 μ M) labeled reporter BACE1 was mixed with ROCK2 in a concentration to achieve 25–50% complex formation. Subsequently, increasing amounts of unlabeled peptide or protein were added and the FP signal was measured as described earlier for direct affinity determination experiments. The dissociation constant (K_d) was determined by fitting the data to the competition-binding Morrison equation [51] with GraphPad Prism 9 (GraphPad Software, San Diego, CA, USA). Titration experiments were carried out in duplicates, and the average FP signal was used for fitting the data.

4.5. Surface Plasmon Resonance (SPR)

SPR experiments were measured on a Biacore X (Cytiva, Danaher, Washington, DC, USA) two-channel SPR system using CM5 sensors. Full-length ROCK2 protein was immobilized using an Amine Coupling Kit. The surface matrices were activated by a 7 min injection of an aqueous solution of 0.2 M 1-ethyl-3-(3-dimethylpropyl)-carbodiimide and 0.05 M N-hydroxysuccinimide. Then ROCK2 at 50 μ g/mL concentration in 0.01 M Na-acetate (pH 5) was injected into the sensor cell (30–60 μ L). Remaining N-hydroxysuccinimide-ester groups were inactivated by an injection of 35 μ L 0.1 M ethanolamine-HCl. Experiments were executed in an HBS-EP buffer (10 mM HEPES, 0.15 M NaCl, 3 mM EDTA and 0.005% Surfactant P20 (= Tween 20) with a pH of 7.4). During the analysis, the flow rate was 10 μ L/min for both the association and dissociation phases. BACE1CD and APP were used at 7 μ M, while MgATP was used at 100 μ M concentrations.

4.6. Modeling of the Binary Complexes

Structures of ROCK2-BACE1 and ROCK2-APP_{646–695} complexes were predicted using AlphaFold-Multimer [39] as implemented in ColabFold [40]. Version 1.3.0 of ColabFold was run locally as implemented in LocalColabFold (<https://github.com/YoshitakaMo/localcolabfold>, accessed on 26 September 2022). The number of recycling iterations was set to 3. Five models were generated, and the best model, as ranked by the interface pTM score, was selected. Models were built with both the homodimeric and monomeric forms of ROCK2. Since no interaction was found between the substrate (BACE1 or APP_{646–695}) and the distant ROCK2 subunit, we present the models with the monomeric ROCK2 in this paper.

Author Contributions: Conceptualization, I.H. and P.Z.; methodology, I.H., B.M.V. and A.S.; validation, B.M.V.; formal analysis, I.H.; investigation, I.H., B.M.V. and A.S.; writing—original draft preparation, I.H. and B.M.V.; writing—review and editing, I.H., A.S. and P.Z.; visualization, I.H., B.M.V. and A.S.; supervision, P.Z.; project administration, I.H.; funding acquisition, A.S. and P.Z. All authors have read and agreed to the published version of the manuscript.

Funding: This work has been supported by the grants K134711 (OTKA) and K128262 (OTKA) provided by the National Research, Development and Innovation Office of Hungary (NKFIH).

Institutional Review Board Statement: Not applicable.

Informed Consent Statement: Not applicable.

Data Availability Statement: All datasets generated for this study are included in this article.

Acknowledgments: We thank Peter Gál (RCNS, Budapest, Hungary) for his support and continuous attention during this project. We also thank Gedeon Richter Plc. for the financial support. We are indebted to István Greiner and Tamás Pázmány for their help and encouragement during this work.

Conflicts of Interest: The authors declare no conflict of interest.

References

1. Hampel, H.; Hardy, J.; Blennow, K.; Chen, C.; Perry, G.; Kim, S.H.; Villemagne, V.L.; Aisen, P.; Vendruscolo, M.; Iwatsubo, T.; et al. The Amyloid- β Pathway in Alzheimer's Disease. *Mol. Psychiatry* **2021**, *26*, 5481–5503. [[CrossRef](#)]
2. Walsh, S.; Merrick, R.; Milne, R.; Brayne, C. Aducanumab for Alzheimer's Disease? *BMJ* **2021**, *374*, n1682. [[CrossRef](#)] [[PubMed](#)]
3. Kojro, E.; Fahrenholz, F. The Non-Amyloidogenic Pathway: Structure and Function of Alpha-Secretases. *Subcell Biochem.* **2005**, *38*, 105–127. [[CrossRef](#)]
4. Cole, S.L.; Vassar, R. The Alzheimer's Disease β -Secretase Enzyme, BACE1. *Mol. Neurodegener.* **2007**, *2*, 22. [[CrossRef](#)]
5. Bai, X.; Yan, C.; Yang, G.; Lu, P.; Ma, D.; Sun, L.; Zhou, R.; Scheres, S.H.W.; Shi, Y. An Atomic Structure of Human γ -Secretase. *Nature* **2015**, *525*, 212–217. [[CrossRef](#)]
6. Choy, R.W.-Y.; Cheng, Z.; Schekman, R. Amyloid Precursor Protein (APP) Traffics from the Cell Surface via Endosomes for Amyloid β ($A\beta$) Production in the Trans-Golgi Network. *Proc. Natl. Acad. Sci. USA* **2012**, *109*, E2077–E2082. [[CrossRef](#)]
7. Zhang, T.; Chen, D.; Lee, T.H. Phosphorylation Signaling in APP Processing in Alzheimer's Disease. *Int. J. Mol. Sci.* **2019**, *21*, E209. [[CrossRef](#)]
8. Herskowitz, J.H.; Feng, Y.; Mattheyses, A.L.; Hales, C.M.; Higginbotham, L.A.; Duong, D.M.; Montine, T.J.; Troncoso, J.C.; Thambisetty, M.; Seyfried, N.T.; et al. Pharmacologic Inhibition of ROCK2 Suppresses Amyloid- β Production in an Alzheimer's Disease Mouse Model. *J. Neurosci.* **2013**, *33*, 19086–19098. [[CrossRef](#)] [[PubMed](#)]
9. Feng, Y.; Yin, Y.; Weiser, A.; Griffin, E.; Cameron, M.D.; Lin, L.; Ruiz, C.; Schürer, S.C.; Inoue, T.; Rao, P.V.; et al. Discovery of Substituted 4-(Pyrazol-4-Yl)-Phenylbenzodioxane-2-Carboxamides as Potent and Highly Selective Rho Kinase (ROCK-II) Inhibitors. *J. Med. Chem.* **2008**, *51*, 6642–6645. [[CrossRef](#)] [[PubMed](#)]
10. Loirand, G. Rho Kinases in Health and Disease: From Basic Science to Translational Research. *Pharmacol. Rev.* **2015**, *67*, 1074–1095. [[CrossRef](#)] [[PubMed](#)]
11. Wen, W.; Liu, W.; Yan, J.; Zhang, M. Structure Basis and Unconventional Lipid Membrane Binding Properties of the PH-C1 Tandem of Rho Kinases. *J. Biol. Chem.* **2008**, *283*, 26263–26273. [[CrossRef](#)] [[PubMed](#)]
12. Truebestein, L.; Elsner, D.J.; Fuchs, E.; Leonard, T.A. A Molecular Ruler Regulates Cytoskeletal Remodelling by the Rho Kinases. *Nat. Commun.* **2015**, *6*, 10029. [[CrossRef](#)] [[PubMed](#)]
13. Hajdú, I.; Szilágyi, A.; Végh, B.M.; Wacha, A.; Györffy, D.; Grácz, É.; Somogyi, M.; Gál, P.; Závodszy, P. Ligand-Induced Conformational Rearrangements Regulate the Switch between Membrane-Proximal and Distal Functions of Rho Kinase 2. *Commun. Biol.* **2020**, *3*, 721. [[CrossRef](#)]
14. Goate, A.; Chartier-Harlin, M.C.; Mullan, M.; Brown, J.; Crawford, F.; Fidani, L.; Giuffra, L.; Haynes, A.; Irving, N.; James, L. Segregation of a Missense Mutation in the Amyloid Precursor Protein Gene with Familial Alzheimer's Disease. *Nature* **1991**, *349*, 704–706. [[CrossRef](#)] [[PubMed](#)]
15. Rohan de Silva, H.A.; Jen, A.; Wickenden, C.; Jen, L.S.; Wilkinson, S.L.; Patel, A.J. Cell-Specific Expression of Beta-Amyloid Precursor Protein Isoform mRNAs and Proteins in Neurons and Astrocytes. *Brain Res. Mol. Brain Res.* **1997**, *47*, 147–156. [[CrossRef](#)] [[PubMed](#)]
16. Vassar, R.; Bennett, B.D.; Babu-Khan, S.; Kahn, S.; Mendiaz, E.A.; Denis, P.; Teplow, D.B.; Ross, S.; Amarante, P.; Loeloff, R.; et al. Beta-Secretase Cleavage of Alzheimer's Amyloid Precursor Protein by the Transmembrane Aspartic Protease BACE. *Science* **1999**, *286*, 735–741. [[CrossRef](#)]
17. Sastre, M.; Steiner, H.; Fuchs, K.; Capell, A.; Multhaup, G.; Condron, M.M.; Teplow, D.B.; Haass, C. Presenilin-Dependent Gamma-Secretase Processing of Beta-Amyloid Precursor Protein at a Site Corresponding to the S3 Cleavage of Notch. *EMBO Rep.* **2001**, *2*, 835–841. [[CrossRef](#)]
18. Zhao, G.; Mao, G.; Tan, J.; Dong, Y.; Cui, M.-Z.; Kim, S.-H.; Xu, X. Identification of a New Presenilin-Dependent Zeta-Cleavage Site within the Transmembrane Domain of Amyloid Precursor Protein. *J. Biol. Chem.* **2004**, *279*, 50647–50650. [[CrossRef](#)] [[PubMed](#)]
19. De Strooper, B.; Saftig, P.; Craessaerts, K.; Vanderstichele, H.; Guhde, G.; Annaert, W.; Von Figura, K.; Van Leuven, F. Deficiency of Presenilin-1 Inhibits the Normal Cleavage of Amyloid Precursor Protein. *Nature* **1998**, *391*, 387–390. [[CrossRef](#)]
20. Lee, M.-S.; Kao, S.-C.; Lemere, C.A.; Xia, W.; Tseng, H.-C.; Zhou, Y.; Neve, R.; Ahljianian, M.K.; Tsai, L.-H. APP Processing Is Regulated by Cytoplasmic Phosphorylation. *J. Cell Biol.* **2003**, *163*, 83–95. [[CrossRef](#)]
21. Vieira, S.I.; Rebelo, S.; Domingues, S.C.; da Cruz e Silva, E.F.; da Cruz e Silva, O.A.B. S655 Phosphorylation Enhances APP Secretory Traffic. *Mol. Cell. Biochem.* **2009**, *328*, 145–154. [[CrossRef](#)]
22. Hu, Y.-B.; Ren, R.-J.; Zhang, Y.-F.; Huang, Y.; Cui, H.-L.; Ma, C.; Qiu, W.-Y.; Wang, H.; Cui, P.-J.; Chen, H.-Z.; et al. Rho-Associated Coiled-Coil Kinase 1 Activation Mediates Amyloid Precursor Protein Site-Specific Ser655 Phosphorylation and Triggers Amyloid Pathology. *Aging Cell* **2019**, *18*, e13001. [[CrossRef](#)]
23. Aplin, A.E.; Gibb, G.M.; Jacobsen, J.S.; Gallo, J.M.; Anderton, B.H. In Vitro Phosphorylation of the Cytoplasmic Domain of the Amyloid Precursor Protein by Glycogen Synthase Kinase-3beta. *J. Neurochem.* **1996**, *67*, 699–707. [[CrossRef](#)]
24. Iijima, K.; Ando, K.; Takeda, S.; Satoh, Y.; Seki, T.; Itohara, S.; Greengard, P.; Kirino, Y.; Nairn, A.C.; Suzuki, T. Neuron-Specific Phosphorylation of Alzheimer's Beta-Amyloid Precursor Protein by Cyclin-Dependent Kinase 5. *J. Neurochem.* **2000**, *75*, 1085–1091. [[CrossRef](#)] [[PubMed](#)]

25. Standen, C.L.; Brownlees, J.; Grierson, A.J.; Kesavapany, S.; Lau, K.F.; McLoughlin, D.M.; Miller, C.C. Phosphorylation of Thr(668) in the Cytoplasmic Domain of the Alzheimer's Disease Amyloid Precursor Protein by Stress-Activated Protein Kinase 1b (Jun N-Terminal Kinase-3). *J. Neurochem.* **2001**, *76*, 316–320. [[CrossRef](#)]
26. Kim, B.M.; You, M.-H.; Chen, C.-H.; Suh, J.; Tanzi, R.E.; Ho Lee, T. Inhibition of Death-Associated Protein Kinase 1 Attenuates the Phosphorylation and Amyloidogenic Processing of Amyloid Precursor Protein. *Hum. Mol. Genet.* **2016**, *25*, 2498–2513. [[CrossRef](#)] [[PubMed](#)]
27. Chen, Z.-C.; Zhang, W.; Chua, L.-L.; Chai, C.; Li, R.; Lin, L.; Cao, Z.; Angeles, D.C.; Stanton, L.W.; Peng, J.-H.; et al. Phosphorylation of Amyloid Precursor Protein by Mutant LRRK2 Promotes AICD Activity and Neurotoxicity in Parkinson's Disease. *Sci. Signal.* **2017**, *10*, eaam6790. [[CrossRef](#)] [[PubMed](#)]
28. Lee, Y.; Lee, J.S.; Lee, K.J.; Turner, R.S.; Hoe, H.-S.; Pak, D.T.S. Polo-like Kinase 2 Phosphorylation of Amyloid Precursor Protein Regulates Activity-Dependent Amyloidogenic Processing. *Neuropharmacology* **2017**, *117*, 387–400. [[CrossRef](#)]
29. Zambrano, N.; Bruni, P.; Minopoli, G.; Mosca, R.; Molino, D.; Russo, C.; Schettini, G.; Sudol, M.; Russo, T. The Beta-Amyloid Precursor Protein APP Is Tyrosine-Phosphorylated in Cells Expressing a Constitutively Active Form of the Abl Protooncogene. *J. Biol. Chem.* **2001**, *276*, 19787–19792. [[CrossRef](#)]
30. Poulsen, E.T.; Iannuzzi, F.; Rasmussen, H.F.; Maier, T.J.; Enghild, J.J.; Jørgensen, A.L.; Matrone, C. An Aberrant Phosphorylation of Amyloid Precursor Protein Tyrosine Regulates Its Trafficking and the Binding to the Clathrin Endocytic Complex in Neural Stem Cells of Alzheimer's Disease Patients. *Front. Mol. Neurosci.* **2017**, *10*, 59. [[CrossRef](#)]
31. Rebelo, S.; Vieira, S.I.; Esselmann, H.; Wiltfang, J.; da Cruz e Silva, E.F.; da Cruz e Silva, O.A.B. Tyrosine 687 Phosphorylated Alzheimer's Amyloid Precursor Protein Is Retained Intracellularly and Exhibits a Decreased Turnover Rate. *Neurodegener. Dis.* **2007**, *4*, 78–87. [[CrossRef](#)]
32. Wang, H.; Li, R.; Shen, Y. β -Secretase: Its Biology as a Therapeutic Target in Diseases. *Trends Pharmacol. Sci.* **2013**, *34*, 215–225. [[CrossRef](#)] [[PubMed](#)]
33. Hampel, H.; Vassar, R.; De Strooper, B.; Hardy, J.; Willem, M.; Singh, N.; Zhou, J.; Yan, R.; Vanmechelen, E.; De Vos, A.; et al. The β -Secretase BACE1 in Alzheimer's Disease. *Biol. Psychiatry* **2021**, *89*, 745–756. [[CrossRef](#)] [[PubMed](#)]
34. Pastorino, L.; Ikin, A.F.; Nairn, A.C.; Pursnani, A.; Buxbaum, J.D. The Carboxyl-Terminus of BACE Contains a Sorting Signal That Regulates BACE Trafficking but Not the Formation of Total A β . *Mol. Cell. Neurosci.* **2002**, *19*, 175–185. [[CrossRef](#)]
35. Walter, J.; Fluhrer, R.; Hartung, B.; Willem, M.; Kaether, C.; Capell, A.; Lammich, S.; Multhaup, G.; Haass, C. Phosphorylation Regulates Intracellular Trafficking of Beta-Secretase. *J. Biol. Chem.* **2001**, *276*, 14634–14641. [[CrossRef](#)]
36. von Arnim, C.A.F.; von Einem, B.; Weber, P.; Wagner, M.; Schwanzar, D.; Spoelgen, R.; Strauss, W.L.S.; Schneckenburger, H. Impact of Cholesterol Level upon APP and BACE Proximity and APP Cleavage. *Biochem. Biophys. Res. Commun.* **2008**, *370*, 207–212. [[CrossRef](#)]
37. Radzimanowski, J.; Simon, B.; Sattler, M.; Beyreuther, K.; Sinning, I.; Wild, K. Structure of the Intracellular Domain of the Amyloid Precursor Protein in Complex with Fe65-PTB2. *EMBO Rep.* **2008**, *9*, 1134–1140. [[CrossRef](#)] [[PubMed](#)]
38. Jumper, J.; Evans, R.; Pritzel, A.; Green, T.; Figurnov, M.; Ronneberger, O.; Tunyasuvunakool, K.; Bates, R.; Žídek, A.; Potapenko, A.; et al. Highly Accurate Protein Structure Prediction with AlphaFold. *Nature* **2021**, *596*, 583–589. [[CrossRef](#)]
39. Evans, R.; O'Neill, M.; Pritzel, A.; Antropova, N.; Senior, A.; Green, T.; Žídek, A.; Bates, R.; Blackwell, S.; Yim, J.; et al. Protein Complex Prediction with AlphaFold-Multimer. *BioRxiv* **2021**. [[CrossRef](#)]
40. Mirdita, M.; Schütze, K.; Moriwaki, Y.; Heo, L.; Ovchinnikov, S.; Steinegger, M. ColabFold: Making Protein Folding Accessible to All. *Nat. Methods* **2022**, *19*, 679–682. [[CrossRef](#)]
41. Das, B.; Yan, R. A Close Look at BACE1 Inhibitors for Alzheimer's Disease Treatment. *CNS Drugs* **2019**, *33*, 251–263. [[CrossRef](#)] [[PubMed](#)]
42. Julian, L.; Olson, M.F. Rho-Associated Coiled-Coil Containing Kinases (ROCK): Structure, Regulation, and Functions. *Small GTPases* **2014**, *5*, e29846. [[CrossRef](#)]
43. Kümper, S.; Mardakheh, F.K.; McCarthy, A.; Yeo, M.; Stamp, G.W.; Paul, A.; Worboys, J.; Sadok, A.; Jørgensen, C.; Guichard, S.; et al. Rho-Associated Kinase (ROCK) Function Is Essential for Cell Cycle Progression, Senescence and Tumorigenesis. *Elife* **2016**, *5*, e12994. [[CrossRef](#)] [[PubMed](#)]
44. Cutler, C.; Lee, S.J.; Arai, S.; Rotta, M.; Zoghi, B.; Lazaryan, A.; Ramakrishnan, A.; DeFilipp, Z.; Salhotra, A.; Chai-Ho, W.; et al. Belumosudil for Chronic Graft-versus-Host Disease after 2 or More Prior Lines of Therapy: The ROCKstar Study. *Blood* **2021**, *138*, 2278–2289. [[CrossRef](#)]
45. Brear, P.; Hyvönen, M. Crystal Structure of the Rho-Associated Coiled-Coil Kinase 2 Inhibitor Belumosudil Bound to CK2 α . *Acta Crystallogr. F Struct. Biol. Commun.* **2022**, *78*, 348–353. [[CrossRef](#)]
46. Akama, T.; Dong, C.; Virtucio, C.; Sullivan, D.; Zhou, Y.; Zhang, Y.-K.; Rock, F.; Freund, Y.; Liu, L.; Bu, W.; et al. Linking Phenotype to Kinase: Identification of a Novel Benzoxaborole Hinge-Binding Motif for Kinase Inhibition and Development of High-Potency Rho Kinase Inhibitors. *J. Pharmacol. Exp. Ther.* **2013**, *347*, 615–625. [[CrossRef](#)]
47. Kinoshita, A.; Fukumoto, H.; Shah, T.; Whelan, C.M.; Irizarry, M.C.; Hyman, B.T. Demonstration by FRET of BACE Interaction with the Amyloid Precursor Protein at the Cell Surface and in Early Endosomes. *J. Cell Sci.* **2003**, *116*, 3339–3346. [[CrossRef](#)]
48. Das, U.; Scott, D.A.; Ganguly, A.; Koo, E.H.; Tang, Y.; Roy, S. Activity-Induced Convergence of APP and BACE-1 in Acidic Microdomains via an Endocytosis-Dependent Pathway. *Neuron* **2013**, *79*, 447–460. [[CrossRef](#)]

49. Somogyi, M.; Szimler, T.; Baksa, A.; Vég, B.M.; Bakos, T.; Paréj, K.; Ádám, C.; Zsigmond, Á.; Megyeri, M.; Flachner, B.; et al. A Versatile Modular Vector Set for Optimizing Protein Expression among Bacterial, Yeast, Insect and Mammalian Hosts. *PLoS ONE* **2019**, *14*, e0227110. [[CrossRef](#)]
50. Maina, C.V.; Riggs, P.D.; Grandea, A.G.; Slatko, B.E.; Moran, L.S.; Tagliamonte, J.A.; McReynolds, L.A.; Guan, C.D. An Escherichia Coli Vector to Express and Purify Foreign Proteins by Fusion to and Separation from Maltose-Binding Protein. *Gene* **1988**, *74*, 365–373. [[CrossRef](#)] [[PubMed](#)]
51. Morrison, J.F. Kinetics of the Reversible Inhibition of Enzyme-Catalysed Reactions by Tight-Binding Inhibitors. *Biochim. Biophys. Acta (BBA) Enzymol.* **1969**, *185*, 269–286. [[CrossRef](#)]

Disclaimer/Publisher's Note: The statements, opinions and data contained in all publications are solely those of the individual author(s) and contributor(s) and not of MDPI and/or the editor(s). MDPI and/or the editor(s) disclaim responsibility for any injury to people or property resulting from any ideas, methods, instructions or products referred to in the content.